frontiers in
NEURAL CIRCUITS

ORIGINAL RESEARCH ARTICLE
published: 23 August 2011
doi: 10.3389/fncir.2011.00009

Delta protocadherin 10 is regulated by activity in the mouse main olfactory system

Eric O. Williams, Heather M. Sickles, Alison L. Dooley, Sierra Palumbos, Adam J. Bisogni and David M. Lin*

Department of Biomedical Sciences, Cornell University, Ithaca, NY, USA

Edited by:
Leslie B. Vosshall, Rockefeller University, USA

Reviewed by:
Brian Key, The University of Queensland, Australia
Leonardo Belluscio, National Institutes of Health, USA

****Correspondence:***
David M. Lin, Department of Biomedical Sciences, Cornell University, T2 006A VRT, Tower Road, Ithaca, NY 14853, USA.
e-mail: dml45@cornell.edu

Olfactory sensory neurons (OSNs) are thought to use activity-dependent and independent mechanisms to regulate the expression of axon guidance genes. However, defining the molecular mechanisms that underlie activity-dependent OSN guidance has remained elusive. Only a handful of genes have been identified whose expression is regulated by activity. Interestingly, all of these genes have been shown to play a role in OSN axon guidance, underscoring the importance of identifying other genes regulated by activity. Furthermore, studies suggest that more than one downstream mechanism regulates target gene expression. Thus, both the number of genes regulated by activity and how many total mechanisms control this expression are not well understood. Here we identify *delta protocadherin 10* (*pcdh10*) as a gene regulated by activity. *Delta* protocadherins are members of the cadherin superfamily, and *pcdh10* is known to be important for axon guidance during development. We show *pcdh10* is expressed in the nasal epithelium and olfactory bulb in patterns consistent with providing guidance information to OSNs. We use naris occlusion, genetic manipulations, and pharmacological assays to show *pcdh10* can be regulated by activity, consistent with activation via the *cyclic nucleotide-gated* channel. Transgenic analysis confirms a potential role for *pcdh10* in OSN axon guidance.

Keywords: olfactory, activity, axon guidance, *delta* protocadherin, *pcdh10, CNGA2*

INTRODUCTION

During development, each olfactory sensory neuron (OSN) must extend an axon from the nasal epithelium to the olfactory bulb. Within the bulb, each axon will terminate in structures of neuropil called glomeruli. Although there are ~1800 glomeruli, each OSN will terminate within just one glomerulus. Remarkably, this pattern appears highly stereotyped. OSNs expressing a given odorant receptor will reproducibly converge upon glomeruli located at apparently defined positions within the olfactory bulb (Sakano, 2010).

Recent studies suggest that activity may be a critical component of OSN guidance. Loss of spontaneous neuronal activity can delay glomerular formation (Yu et al., 2004). Similarly, mutations in the *hyperpolarization-activated cyclic nucleotide-gated (HCN)* channel can also affect later stages of OSN outgrowth and glomerular morphology (Mobley et al., 2010). However, loss of the *cyclic nucleotide-gated (CNG)* channel, the primary mediator of electrical signaling in OSNs, has apparently minimal effects on the glomerular map (Lin et al., 2000). Why some mutations that affect electrical activity can have a strong effect on OSN guidance while others are more subtle is still unclear.

Perhaps the most significant insight regarding activity and OSN guidance has been gained from studies manipulating cAMP signaling. It has long been known the specific odorant receptor expressed by an OSN plays a part in guidance (Mombaerts et al., 1996). Transgenic and knockout studies showed altering production of cAMP levels downstream of the receptor can affect OSN targeting (Imai et al., 2006; Zou et al., 2007). These studies implicated two different receptor-dependent mechanisms. At early stages of neuronal outgrowth, alterations in levels of PKA can affect expression of genes such as *semaphorin3A*. At later stages of development, activity mediated via the *CNG* channel appears to regulate genes such as *kirrel2/3*. These studies have led to a two-stage model where the initial phase of OSN guidance is mediated in part by genes regulated by PKA while terminal stages of guidance are determined in part by genes regulated via the *CNG* channel (Imai and Sakano, 2008). Thus, changes in activity, broadly defined to include electrical signaling as well as second messengers (Zou et al., 2009), can affect OSN axon guidance.

But since these initial studies, only one other gene (*BIG2*) has been functionally proven to be affected by changes in activity (Kaneko-Goto et al., 2008). In total, less than 10 genes are known to be regulated by either pathway (Sakano, 2010). Furthermore, studies on *BIG2* suggest more than one mechanism exists to regulate target gene expression by the *CNG* channel (Imai and Sakano, 2008; Kaneko-Goto et al., 2008). In order to better understand the role of activity in OSN guidance, and to determine how many pathways exist to regulate the expression of genes by activity, it is critical to first identify additional candidate genes.

Here we show *protocadherin 10* (*pcdh10*) is regulated by activity in the mouse olfactory epithelium. *Pcdh10* is a member of the *delta* protocadherin subfamily, which in turn is part of the cadherin superfamily (Redies et al., 2005). Although there are some 50 different protocadherins, mutant analysis has proven loss of *pcdh10* alone can influence different aspects of development and postnatal life. Deletion analysis of *pcdh10* in mice revealed significant defects in axon guidance within the cortex (Uemura et al., 2007). In *pcdh10* mutants, striatal neuron outgrowth was affected. Loss of striatal neuron pathways in turn appears to produce defects in corticothalamic and thalamocortical projections. Furthermore, genome wide association studies have implicated *pcdh10* in autism

(Morrow et al., 2008), consistent with a role in nervous system development. In this same study, *pcdh10* was described as being up-regulated in hippocampal cultures under conditions that increase neuronal activity. These data collectively argue that *pcdh10* is important for neural development and can be regulated by activity.

Here we examine the regulation of *pcdh10* expression in the mouse olfactory system. We show *pcdh10* is expressed in a mosaic pattern within the epithelium, consistent with a role in axon guidance or synaptogenesis in OSNs. We use naris occlusion and a knockout mutation in the *cyclic nucleotide-gated channel subunit A2 (CNGA2)* channel to show reductions in odorant-evoked activity can negatively affect *pcdh10* expression. We further demonstrate using epithelial explants that addition of forskolin can increase *pcdh10* expression. Finally, we show in a transgenic model that misexpression of *pcdh10* in OSNs has an effect on late-stage axonal phenotypes.

MATERIALS AND METHODS

ANIMAL USE

All protocols for treatment and breeding of animals were approved by the Cornell IACUC. Swiss-Webster and C57Bl/6 mice were used for expression studies and naris occlusion assays. The day a vaginal plug was observed was considered day P0.5.

NARIS OCCLUSION

Occlusion was accomplished by cauterizing one nostril of P0 pups briefly with a soldering iron set to 350°C. Closure was monitored daily and animals re-cauterized as needed. Animals were sacrificed 12–15 days after occlusion.

GENERATION OF TRANSGENIC MICE

About 5.4 kb of the rat *olfactory marker protein* (*OMP)* promoter upstream of the ATG was fused to a *pcdh10* isoform (NM011043.2). An internal ribosome entry site was inserted at the 3′ end followed by *eGFP* and a bovine growth hormone polyA sequence. Transgenic animals were produced by the Cornell Transgenic Mouse Facility. Four independent inserts were obtained and two were used for analysis.

SINGLE AND DOUBLE-LABEL *IN SITU* HYBRIDIZATION

In situ hybridization was done as previously described (Rodriguez et al., 2008). In brief, 20 μm fresh-frozen cryosections were fixed in 4% paraformaldehyde, washed with PBS, and acetylated with 0.25% acetic anhydride in 0.1 M triethanolamine, pH 8.0. Slides were washed again and blocked for 2 h. Slides were hybridized with digoxigenin and/or biotin-labeled antisense RNA probes for 48 h at 60°C. Slides were washed at 60°C with 5× SSC and then with 0.2× SSC, cooled to room temperature and blocked with TNB reagent (Perkin Elmer). Alkaline phosphatase conjugated anti-digoxigenin antibody was applied to slides (Roche) in block overnight at 4°C. For single color *in situ* hybridizations, slides were washed with B1 buffer (100 mM Tris pH 7.4, 150 mM NaCl), followed by B3 buffer (100 mM Tris pH 9.5, 50 mM $MgCl_2$, 100 mM NaCl) and reacted in NBT/BCIP (Promega).

For double-label fluorescence *in situ* hybridization, bound biotinylated probe was detected using the tyramide signal amplification (TSA) kit as per manufacturer's instructions (Perkin Elmer). Digoxigenin-bound probe was detected with the HNPP kit as per manufacturer's instructions (Roche). To detect both probes, slides were first reacted with the TSA kit, washed in fast red buffer (100 mM Tris pH 8.0, 50 mM $MgCl_2$, 100 mM NaCl), and incubated in Texas Red/HNPP solution at room temperature. The HNPP step was repeated, and slides were rinsed in running tap water for 5 min, mounted in 70% glycerol with DAPI, and analyzed using a Leica LSM 510 Meta confocal microscope. To analyze co-expression, five optical slices (each 3 μm thick) of a given visual field were combined into a z-stack, and all five images assessed for colocalization.

Probe sequences: *pcdh10* (NM_001098170 – nt 856–3000, 3070–3276, 3487–3976), *kirrel2* (NM_172898 – nt 242–1077), *kirrel3* (NM_001190911 – nt 500–1506, 500–2457), *neuropilin-1* (NM_008737 – nt 1203–1787, 1787–2751), *plexinA1* (NM_008881 – nt 485–1371, 752–1788), *MOR28* NM_001170918 (1520–1605), *SR1* (NM_147062 – nt 1027–1122), *OR78* (NM_130866 – nt 1219–2190), *OMP* (IMAGE clone IRAKp961I03127Q).

ANTIBODIES AND IMMUNOHISTOCHEMISTRY

Cyclic nucleotide-gated channel subunit A2 antibody was purchased from Abcam (ab79261). Olfactory bulbs from *CNGA2* heterozygous mice were fixed in 10% neutral buffered formalin overnight and embedded in paraffin. 5μm sections were collected and dried at 37°C overnight. Sections were deparaffinized and microwaved in antigen retrieval buffer (10 mM Tris pH 9.0, 1 mM EDTA, 0.05% Tween 20) 5 × 10 min on low power. Slides were cooled to room temperature and washed in PBST (PBS, 0.05% Tween20). Slides were blocked in TNB before incubation with primary antibody overnight at 4°C. Slides were washed in PBST and incubated with biotinylated goat anti-rabbit antibody (Vector Labs) in TNB at room temperature. Slides were washed in PBST and incubated in streptavidin–HRP (Invitrogen) for 30 min. Signal was visualized with AEC substrate as per manufacturer's instructions (Invitrogen). Antibodies directed against phosphocreb were obtained from Millipore (06-519).

Pcdh10 antibody was produced by Biogenes GmBH (Berlin, Germany). Rabbits were injected with adjuvant and the peptide CSPSRSTDAEHN. *Pcdh10* immunohistochemistry was performed on 20 μm thick fixed or fresh-frozen cryosections. Sections were postfixed in 4% phosphate-buffered paraformaldehyde, washed with PBS, and endogenous peroxidase quenched by incubation in 3% hydrogen peroxide. Slides were washed and antigen retrieval accomplished by heating slides in 10 mM sodium citrate (pH 9.0) for 1 h at 80°C. Slides were washed and blocked in 10% non-fat dried milk containing 10% heat inactivated goat serum. Antibody was incubated overnight at 4°C, and then subsequently at 37°C for an additional 2 h. Secondary and tertiary reactions were performed as described above for the *CNGA2* antibody.

GLOMERULAR MAP

Coronal sections from P0 olfactory bulbs immunostained with *pcdh10* antibody were photographed. The glomerular layer of each image was cropped, inverted, and imported into DeltaViewer 2.1[1]. Sections were manually aligned and reconstructed into three-dimensional images.

[1]http://delta.math.sci.osaka-u.ac.jp/DeltaViewer/DVAbout.html

BETA-GALACTOSIDASE ACTIVITY

Whole mount *lacZ* staining was performed on olfactory bulbs as follows: tissue was dissected and fixed in 2% paraformaldehyde/phosphate buffer for 5 min. Olfactory bulbs were washed in PBS and incubated in staining buffer without X-Gal (10 mM PO_4 buffer pH 7.4, 150 mM NaCl, 1 mM $MgCl_2$, 3 mM ferrous cyanide, 3 mM ferric cyanide, and 0.3% Triton X-100) heated to 37°C. This buffer was then replaced with staining buffer containing 0.2% X-Gal and incubated at 37°C. To quantitate interglomerular distance, olfactory bulbs were fixed in 4% paraformaldehyde and 20 μm cryosections processed for *beta*-galactosidase activity. The interglomerular distance was calculated by counting the number of sections collected between *lacZ* positive glomeruli and multiplying by 20.

EXPLANT CULTURES

P3–P5 epithelia were dissected in ice-cold Modified Eagles Media (Invitrogen) and the cartilage removed. Epithelia were finely minced with a razor blade and digested for 10 min in MEM containing 5 mg/ml dispase, 1mg/ml collagenase IV, 1 mg/ml hyaluronidase, and 50 μg/ml DNAase I, as described (Ronnett et al., 1991). Digests were neutralized with media containing serum (1× MEM, 10% dialyzed FBS, 5% Nu-serum, 1× anti–anti), and strained through a 40-μm cell-strainer (Becton Dickson). Explants were recovered by rinsing with 1× MEM and plated in serum-containing media in a humidified incubator at 37°C with 6% CO_2.

PHARMACOLOGICAL TREATMENTS

To determine phosphocreb induction patterns, explant cultures were incubated with forskolin (Sigma) 16–24 h after plating. To inhibit PKA, RpcAMPs (40 μM, Enzo Life Sciences) was added immediately after plating explants for 16–24 h prior to addition of forskolin (20 μM) for 1 h.

QUANTITATIVE RT-PCR

Quantitative RT-PCR was performed using an ABI7500 system. To generate substrate for the qRT-PCR reaction, total RNA was isolated from explant cultures (1–2 μg total per culture) and reverse transcribed using oligo-dT and Superscript III (Invitrogen) as per manufacturer's instructions. Primers for qRT-PCR were designed with primerbank[2]. The endogenous control was *ribosomal protein like 19 (rpl19)*. 2× master mix containing low Rox was purchased from Quanta Biosystems, and the reaction performed according to manufacturer's instruction. Relative expression levels were determined using the 2^{-ddCt} approach. SE was calculated from the technical replicates for each gene. Primer sequences used are as follows:

Kirrel2	CACCAGCCTTTCTGAGGGG	GGCTTCCACTAGGAACCTGC
Kirrel3	AGAACACCATTCAACTCCAACC	CTCCCGCTCACAAAGCTCAA
OMP	TCCGTCTACCGCCTCGATTT	CGTCTGCCTCATTCCAATCCA
GAP43	TGGTGTCAAGCCGGAAGATAA	GCTGGTGCATCACCCTTCT
Pcdh10	GGTTCCCATCACCACAATCAG	CAGCCTTACCTCGTTGGACAA
Rpl19	ATGAGTATGCTCAGGCTACAGA	GCATTGGCGATTTCATTGGTC

[2]http://pga.mgh.harvard.edu/primerbank/

PIXEL INTENSITY

JPEG images of sections were imported into ImageJ[3], converted to 8-bit grayscale, and thresholded. Thresholds were defined manually, but were performed blind. Areas of interest were manually determined, and the number of positive pixels determined using the "measure" function. For the naris occlusion analysis, pixel intensity on the occluded side was normalized per section by dividing by the intensity on the open side. Sixteen to 24 sections from three to four separate occlusion experiments were analyzed for each gene. The ratios were then averaged. Because the ratios included values less than and greater than 1, SE was calculated by first log-transforming the data. Student's *t*-test (two-tailed) was then performed on the transformed data, and a *p*-value calculated. For the *CNGA2* pixel analysis, 35–61 sections were analyzed per gene from three separate *CNGA2* mutants and controls. This analysis was performed blind. Intensity values for any given gene were averaged for each animal, which was then normalized to a littermate matched control. Each pair (mutant and control) were processed simultaneously, and reacted for the same amount of time prior to the analysis. The three ratios for any given gene were then averaged. SE and *p*-values were calculated as described above for the naris occlusion.

RESULTS

PCDH10 IS EXPRESSED IN SUBSETS OF OSNS IN THE EPITHELIUM AND IN SPATIALLY DEFINED LOCATIONS WITHIN THE OLFACTORY BULB

We previously found two other *delta* protocadherins (*pcdh7* and *pcdh17*) are expressed by subsets of OSNs, consistent with a role in guidance and/or synaptogenesis (Williams et al., 2007). As *pcdh10*, another *delta* family member, has been functionally proven to mediate axon guidance in the brain (Uemura et al., 2007), we examined the expression of *pcdh10* in the nasal epithelium and olfactory bulb.

Within the epithelium, *pcdh10* is not detectably expressed by *in situ* hybridization prior to ~E15. At E17.5, *pcdh10* is expressed by subsets of OSNs (**Figures 1A,B**; compare with expression of *OMP*, **Figure 1C**). This distribution is not even throughout the epithelium, but appears more intense along the medial aspect. Expression is also noticeably variable, with strong expression in some OSNs and weaker, more diffuse signal in others. As the animal matures, the bulk of *pcdh10* expression begins to shift more laterally. In the adult, *pcdh10* is expressed most strongly along the ventrolateral epithelium, although the original expression pattern along the dorsomedial aspect can still be identified (**Figure 1D**).

Within the olfactory bulb, *pcdh10* labels a specific subdomain along the dorsolateral surface at E14.5 (**Figure 1E**). This expression pattern is reminiscent of that observed for *pcdh7* and *pcdh17*, which label complementary domains in the olfactory bulb (Williams et al., 2007). Unlike these other *delta* family members, however, *pcdh10* expression within the bulb becomes more uniform at E17.5 (**Figure 1F**), and is essentially distributed throughout the bulb at postnatal and adult stages (**Figure 1G**).

Next we raised an antibody against *pcdh10*. Expression was clearly detectable in glomeruli, consistent with axonal OSN expression. However, we could not reliably detect axonal expression. Because of this, it is possible that some of our signal within glomeruli is due to mitral or periglomerular expression. In keeping

[3]http://rsb.info.nih.gov/ij/

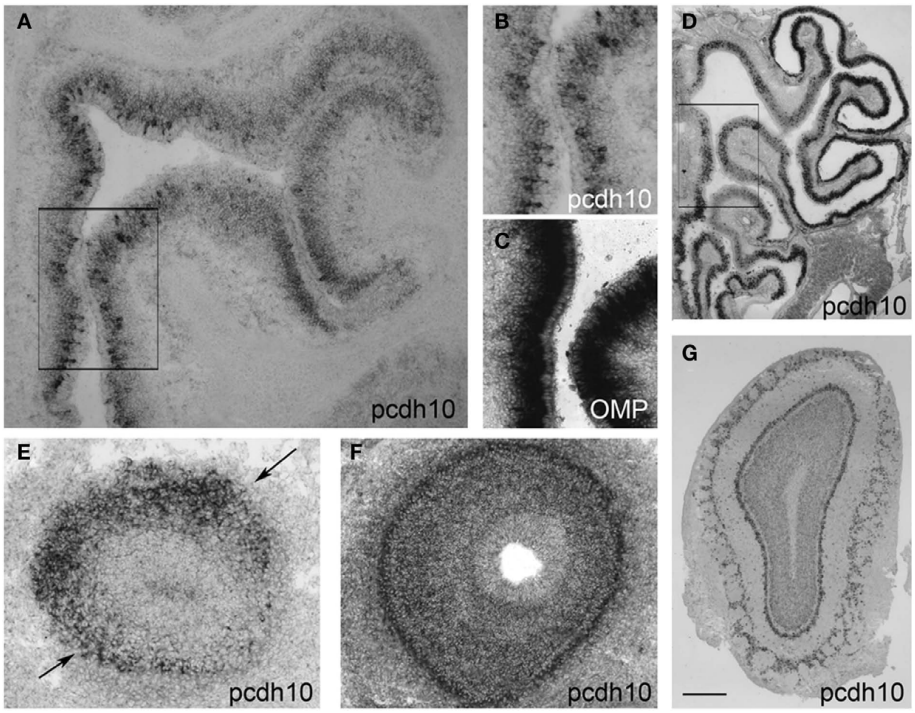

FIGURE 1 | *Pcdh10* expression in the olfactory system. (A) *Pcdh10* is expressed most strongly in the medial epithelium at E17.5. **(B)** Boxed area shown in **(A)** at higher magnification. *Pcdh10* expression is clearly punctate in some OSNs and diffuse in others. Expression levels of *pcdh10* within each OSN also varies. **(C)** *OMP* labels mature OSNs. **(D)** In contrast to embryonic and early postnatal expression, *pcdh10* expression in adulthood is highest in the ventrolateral epithelium. However, the original pattern observed at E17.5 can still be seen in adulthood [compare boxed areas in **(A)** and **(D)**]. In all bulbar images, medial is to the right. **(E)** *Pcdh10* expression in E14.5 olfactory bulb labels a broad domain in the dorsolateral bulb (black arrows), but is weak or absent in the medial bulb. **(F,G)** *Pcdh10* expression in E17.5 **(F)** and adult **(G)** bulbs appears uniformly distributed. Scale bar = 90 μm **(A)**, 30 μm **(B,C)**, 250 μm **(D)**, 50 μm **(E,F)**, 125 μm **(G)**.

with the mosaic expression of *pcdh10* RNA within the epithelium (**Figure 1**), a subset of glomeruli are *pcdh10*-positive at P0 (**Figure 2A**). Interestingly, among *pcdh10*-positive glomeruli, expression appears variable. Some *pcdh10*-positive glomeruli are clearly more intensely stained than others (**Figures 2A,C**). This is reminiscent of the pattern observed in the epithelium, where some OSNs express higher levels of *pcdh10* RNA than others (**Figures 1A,B**). As postnatal stages progresses, the glomerular signal became stronger (P12; **Figure 2B**). Variation in glomerular intensity among *pcdh10*-positive glomeruli is still present, but less obvious than at P0 (**Figure 2D**). A prior report on *pcdh10* expression in the olfactory system (Aoki et al., 2003) showed clear axonal expression and *pcdh10*-positive glomeruli at P7. Unlike this prior study, we were unable to consistently obtain axonal signal. This may be due to differences in antibodies and reaction conditions. However, variable glomerular signal within the bulb was also seen in this prior study.

To determine the pattern of *pcdh10* expression in glomeruli during development, we generated a glomerular map from P0 animals (**Figure 3**; **Movie S1** in Supplementary Material). The map revealed bilateral glomerular expression of *pcdh10* (**Figures 3A,C**). *Pcdh10* was expressed most strongly in the anterior bulb along the lateral aspect, with a slight dorsal bias. In the posterior bulb, however, *pcdh10* was expressed primarily along the medial aspect, with a slight ventral bias. This symmetric expression is highly intriguing, and is reminiscent of the medial–lateral symmetry observed in convergence by OSNs expressing specific odorant receptors.

PCDH10 EXPRESSION IS AFFECTED BY NARIS OCCLUSION

We next looked to determine whether activity affects *pcdh10* expression. We performed naris occlusion to reduce odorant-evoked activity (Kaneko-Goto et al., 2008). In this approach, one naris is surgically closed while the open naris serves as a control. Occlusion presumably reduces access of odors to the epithelium, lowering odorant receptor activity. Naris occlusion was performed at P0, and the animals sacrificed at P12–P15.

We found that *pcdh10* expression was consistently down-regulated in the closed naris as compared to the open naris (**Figures 4A,C**; $n = 10$), suggesting that odorant-evoked activity can regulate *pcdh10* at the transcriptional level. This striking result was highly reminiscent of the phenotype observed for *kirrel2* in a similar naris occlusion paradigm (Kaneko-Goto et al., 2008). In those experiments, expression of *kirrel2* is down-regulated in the occluded naris relative to the open naris. *Kirrel3*, on the other hand, is up-regulated on the occluded side. We therefore also examined *kirrel2*, *kirrel3*, and *OMP* for changes in expression under these conditions. We confirmed *kirrel2* ($n = 13$) is down-regulated in the epithelium of the occluded naris (**Figure 4D**), while *kirrel3* is up-regulated ($n = 10$; **Figure 4E**). *Kirrel3* was not always obviously

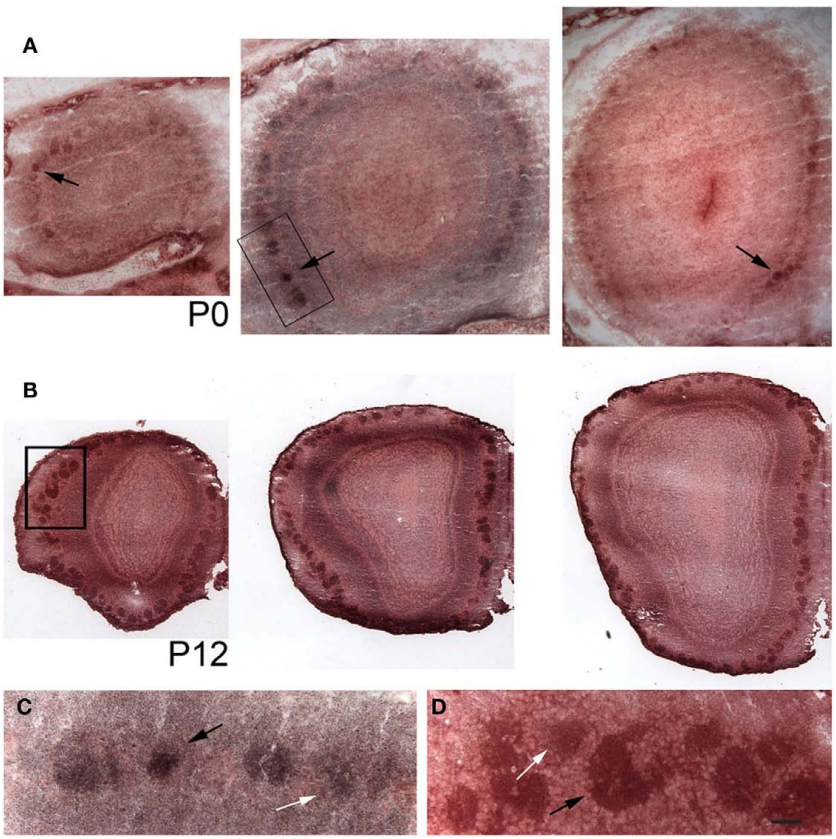

FIGURE 2 | *Pcdh10* is expressed in glomeruli. Cryosections from olfactory bulb immunostained with an antibody directed against *pcdh10*. In all images, medial is to the right. **(A)** Representative sections from the anterior, middle, and posterior olfactory bulb at P0. Glomerular signal at this stage is clearly variable, with some glomeruli (black arrows) showing increased expression relative to others. **(B)** Sections from the anterior, middle, and posterior olfactory bulb at P12. Glomerular signal is in general higher at this age than at P0. **(C)** Higher magnification of boxed area shown in **(A)**. White and black arrows indicate glomeruli with different levels of *pcdh10* expression. **(D)** Higher magnification of boxed area shown in **(B)**. White and black arrows indicate glomeruli with different levels of *pcdh10* expression. Scale bar = 100 μm **(A)**, 200 μm **(B)**, 33 μm **(C,D)**.

up-regulated in all animals ($n = 3$). However, we noted that animals with longer closure times generally showed stronger and more obvious changes in *kirrel3* expression (data not shown). Finally, *OMP* ($n = 11$) expression was apparently unaffected by occlusion (**Figure 4B**). *OMP* is not thought to be regulated by activity.

We quantitated changes in *pcdh10, kirrel2, kirrel3*, and *OMP* by comparing pixel intensity values on the occluded side to the open side in each section (**Figure 4F**). The open side for each section serves as an internal control for each comparison, controlling for variation in reaction times between replicate experiments. Sixteen to 24 sections from four separate experiments were compared for any one gene. Consistent with our qualitative observations, *pcdh10* expression was decreased on the occluded side approximately seven-fold ($p < 0.005$). *Kirrel2* was also reduced to a similar extent ($p < 0.005$). In contrast, *kirrel3* was up-regulated four-fold on the occluded side ($p < 0.005$). *OMP* was essentially unchanged (1.06-fold; $p = 0.08$).

We next performed quantitative RT-PCR on epithelia isolated from occluded animals (**Figure 4G**). Six epithelia were collected and divided in half. Gene expression in the half-epithelium corresponding to the occluded side was compared against that in the open side. Analysis of gene expression in all six epithelia found *kirrel2* and *pcdh10* expression on the occluded side was reduced on average to ~50% of the open side ($p < 0.005$). *Kirrel3* was up-regulated three-fold ($p < 0.005$). Expression of *OMP* was somewhat elevated on the occluded side (1.3-fold, $p < 0.005$). *OMP* expression has been reported to be increased in animals that have been nasally occluded for 3 weeks or more. GAP43 expression appeared unchanged (1.05-fold, $p = 0.98$). Although the exact fold-changes vary, these results parallel our pixel analysis (**Figure 4F**), and show reduction of odorant-evoked activity reduces *pcdh10* expression.

CO-EXPRESSION OF *PCDH10* AND GENES REGULATED BY ACTIVITY

The behavior of *pcdh10* in our nasal occlusion experiments is consistent with regulation of *pcdh10* expression by activity. We next asked whether or not *pcdh10* is co-expressed in OSNs with other genes regulated by activity. *Kirrel2* and *kirrel3* expression is influenced by the *CNG* channel, while *neuropilin-1* and *plexinA1* are thought to be affected by changes in PKA (Imai et al., 2006; Serizawa et al., 2006; Imai and Sakano, 2008). We performed double-label *in situ* hybridization and tested cells

for co-expression by confocal microscopy. We found that 20% of *pcdh10*-positive cells express *neuropilin-1* and 36% express *PlexinA1* (**Table 1**). In contrast, most (96%) *pcdh10*-positive cells express *kirrel2* at E17.5 (**Figures 5A–C**; **Table 1**). The converse, however, is not true. Only 39% (**Figures 5A–C**; $n = 366$) of *kirrel2*-positive OSNs express *pcdh10*. *Kirrel2* is therefore expressed in a larger percentage of OSNs as compared with *pcdh10*. Finally, we found that most (90%) *pcdh10*-positive cells express *OMP* at E17.5 (**Figures 5D–F**; **Table 1**), indicating *pcdh10* is primarily expressed in mature OSNs. This is consistent with the relatively late onset of expression of *pcdh10* (after E15; **Figure 1**), as well as the gradual increase in *pcdh10* expression in glomeruli at postnatal stages (**Figure 2B**).

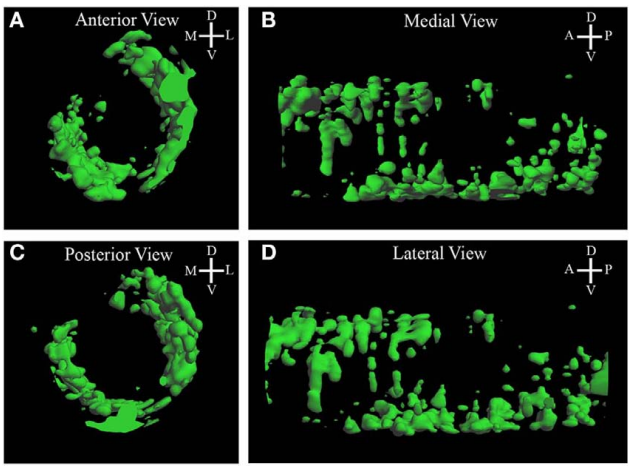

FIGURE 3 | Three-dimensional reconstruction of *Pcdh10* glomerular expression in P0 bulb. (A,D) In the anterior bulb *pcdh10* is detected primarily in lateral glomeruli. **(B,C)** In the posterior olfactory bulb, *pcdh10* is detected primarily in ventral glomeruli.

Kirrel3 is also regulated by activity but in a manner opposite to that of *kirrel2*. Interestingly, we found that *pcdh10* and *kirrel3* also overlap significantly (78%) at P0 (**Table 1**). We therefore asked whether or not OSNs typically express both *kirrels* early in development. At P0, 73% of *kirrel3*-positive OSNs also express *kirrel2* (**Figures 5G–I**; **Table 1**). Glomerular refinement is known to occur during postnatal life, and is dependent upon activity (Zhao and Reed, 2001). As *kirrels* are oppositely regulated by activity, we asked whether or not the proportion of OSNs expressing both *kirrels* changes over time. We found by 2.5 weeks the percentage of OSNs co-expressing *kirrels* drops to 31% (**Table 1**). This change in overlap is also reflected in double-label studies with *pcdh10*. At P0, *kirrel3* is expressed in 78% of *pcdh10*-positive OSNs (**Table 1**). At 2.5 weeks, however, only 20% of these cells express *kirrel3* (**Table 1**). These studies show that regulation of *pcdh10* expression appears to parallel that of *kirrel2*.

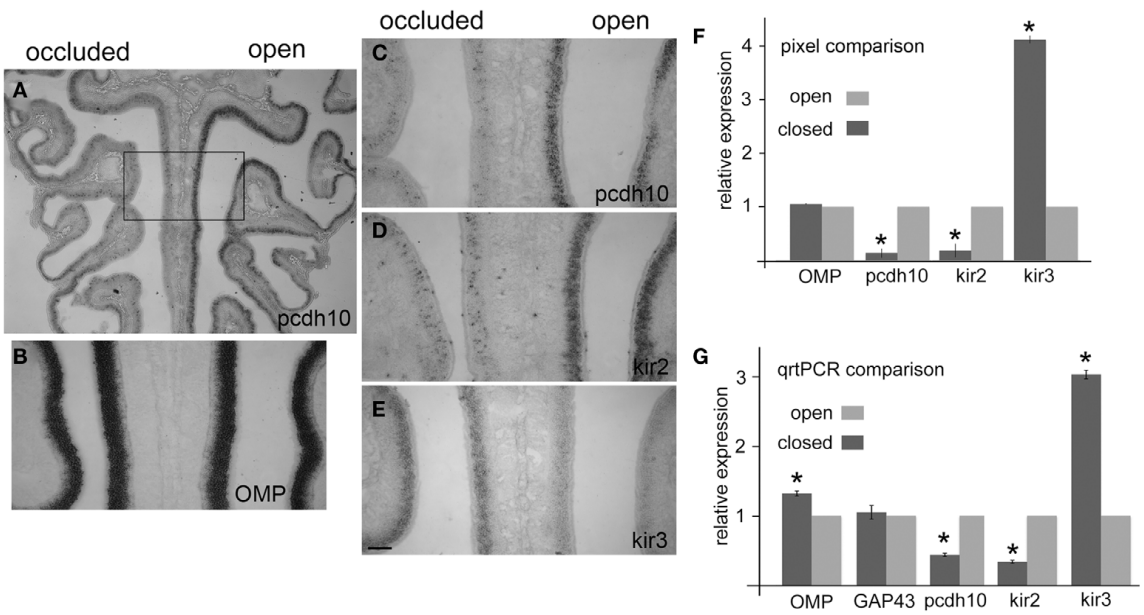

FIGURE 4 | *Pcdh10* epithelial expression is reduced after naris occlusion. In all images, the occluded side is on the left. **(A)** Expression of *pcdh10* on the occluded side is highly reduced relative to the open side. **(B)** *OMP* expression is apparently unaffected by occlusion. **(C)** Higher magnification of boxed area shown in **(A)** shows strong reduction in *pcdh10* expression on the occluded side. **(D)** *Kirrel2* is down-regulated in expression on the occluded side. **(E)** *Kirrel3* expression shows the opposite expression pattern, and is up-regulated on the occluded side. **(F)** Pixel analysis comparing signal intensities on the occluded and open side showed significant reductions in expression for *pcdh10* and *kirrel2*, while *kirrel3* was significantly up-regulated. *OMP* expression was unaffected. *OMP* ($p = 0.08$); *pcdh10, kirrel2, kirrel3* ($p < 0.005$), **(G)** Epithelia from six occluded animals were split in half. Quantitative RT-PCR was performed to compare expression of each half-epithelium from the occluded naris against the corresponding half-epithelium from the open naris. Expression of *OMP* was slightly (1.3×) higher in the occluded side relative to the open side ($p < 0.005$). *GAP43* was unchanged ($p = 0.98$). *Pcdh10* expression on the occluded side was ~50% of the open side ($p < 0.005$), similar to *kirrel2* (35% of open side; $p < 0.005$). *Kirrel3* was increased three-fold on the occluded relative to the open side ($p < 0.005$). Scale bar = 250 μm **(A)** 100 μm **(B–E)**.

PCDH10 EXPRESSION IS REGULATED BY THE *CNG* CHANNEL

Our naris occlusion studies argue that odorant-evoked activity can regulate *pcdh10* expression. To further examine activity and *pcdh10* expression, we next used a mutant defective in the *CNGA2* gene (Lin et al., 2000). The *CNGA2* gene resides on the X chromosome. As a result of random X-inactivation, OSNs will either be *CNGA2*-positive or *CNGA2*-negative in heterozygous mutant females. These OSNs segregate from one another, and can be detected in the bulb as *CNGA2*-positive and -negative glomeruli. *Kirrel2* expression is associated with *CNGA2*-positive glomeruli (Serizawa et al., 2006). To determine if *pcdh10* is similarly co-expressed, we examined serial, 5 μm thick olfactory bulb sections in *CNGA2* heterozygotes for *CNGA2* and *pcdh10* expression (**Figure 6**). We found that *pcdh10*-positive glomeruli co-localized with *CNGA2*-positive glomeruli, consistent with regulation of *pcdh10* expression by activity.

Table 1 | Double-label *in situ* hybridization with *pcdh10* and other activity-regulated genes.

	***OMP* (E17.5)**	***Kirrel2* (E17.5)**	**Nrp1 (E17.5)**	**PlexinA1 (E17.5)**	***Kirrel2* (P0)**	***Kirrel3* (P0)**	***Kirrel2* (2.5 weeks)**	***Kirrel3* (2.5 weeks)**
Pcdh10	90% (*n* = 241)	96% (*n* = 397)	20% (*n* = 105)	36% (*n* = 114)	94% (*n* = 259)	78% (*n* = 261)	89% (*n* = 139)	20% (*n* = 212)
Kirrel3					73% (*n* = 225)		31% (*n* = 198)	

Double-label in situ hybridization was performed with pcdh10 and other genes. Percentage of cells expressing pcdh10 and any given gene are shown, along with the total number of cells assayed by confocal microscopy. Kirrel2 and kirrel3 co-expression was also assessed at P0 and 2.5 weeks.

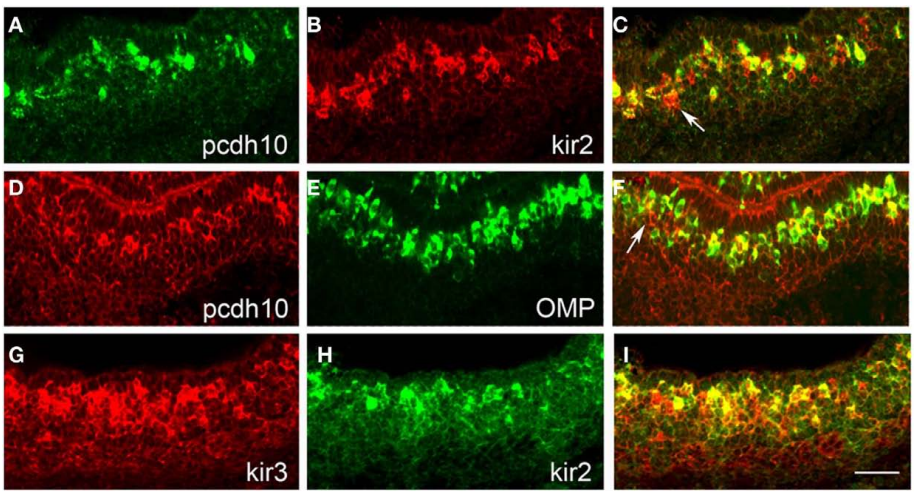

FIGURE 5 | *Pcdh10* is co-expressed with kirrel2/kirrel3. (A–C) Double-label *in situ* hybridization with *pcdh10* [**(A)**; green] and *kirrel2* [**(B)**; red]. Not all *kirrel2*-positive cells express *pcdh10* [**(C)**; white arrow]. **(D–F)** Double-label *in situ* hybridization with *pcdh10* [**(D)**; red] and *OMP* [**(E)**; green]. *Pcdh10* is expressed primarily in mature OSNs, although ~10% appear to be present in immature OSNs [white arrow **(F)** indicates *pcdh10*-positive, *OMP*-negative cell]. **(G–I)** Double-label *in situ* hybridization with *kirrel3* [**(G)**; red] and *kirrel2* [**(H)**; green] at P0 shows significant overlapping expression. Scale bar = 50 μm.

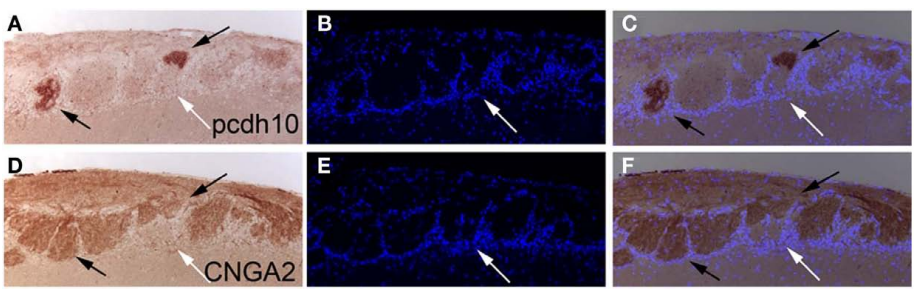

FIGURE 6 | *Pcdh10* expression colocalizes with *CNGA2* in glomeruli. (A–C) *Pcdh10* can be detected in glomeruli within the olfactory bulb (black arrows) in adult *CNGA2* heterozygous animals. DAPI-stained cells are shown in blue. **(D–F)** Alternating section stained with an anti-*CNGA2* antibody demonstrating overlap with *pcdh10*-positive glomeruli. Some glomeruli do not express *pcdh10* or *CNGA2* (white arrows).

We next asked whether or not *CNGA2* mutants had lower levels of *pcdh10* expression within the epithelium relative to littermate controls. Despite extensive efforts, we were unable to generate many postnatal *CNGA2*$^{-/-}$ animals due to severe perinatal lethality (Lin et al., 2000). Some studies implicate odorant activity *in utero* (Todrank et al., 2011). We therefore examined *CNGA2* animals at E16.5 for changes in *pcdh10* and *kirrel2/3* expression. We found significant reduction in expression of both *kirrel2* and *pcdh10* (**Figures 7A–D**; $n = 3$), with fewer cells expressing either gene relative to control. Only subtle differences were seen for *kirrel3* at this age (data not shown).

To confirm our qualitative impressions, we performed pixel analysis to compare signal strength for these genes in *CNGA2* and control epithelia (**Figure 7E**). This quantification was performed blind to eliminate potential selection bias. We found *pcdh10* and *kirrel2* were significantly reduced in expression in *CNGA2* mutants. *Pcdh10* expression was approximately 10% that of control embryos ($p < 0.05$), while *kirrel2* was approximately 2% that of controls ($p < 0.05$). *Kirrel3* was variably increased among the three animals although not in a statistically significant manner ($p = 0.31$). *OMP* expression was essentially equal between mutants and controls (95% of control expression in mutants; $p = 0.69$). These results confirm prior studies on *kirrel2*/3, *Eph/ephrin A5*, and *BIG2*, and extend them by identifying *pcdh10* as a gene whose expression can also be regulated by the *CNG* channel.

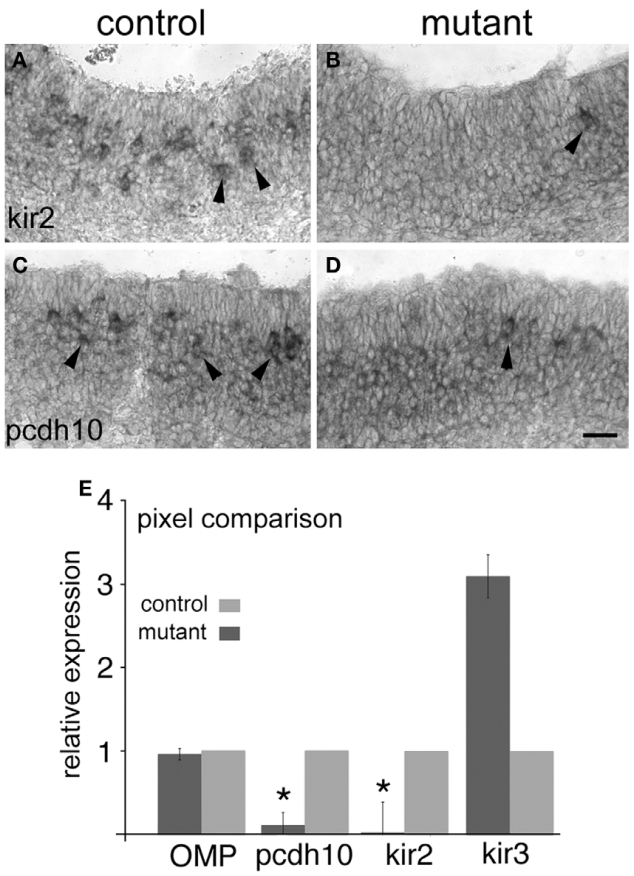

FIGURE 7 | *Pcdh10* is reduced in expression in *CNGA2* mutants. (A) Expression of *kirrel2* in epithelia (arrowheads) of control *CNGA2*$^{+/+}$ littermate at E16.5. **(B)** Expression of *kirrel2* in a *CNGA2*$^{-/-}$ mutant animal (arrowhead) is reduced relative to control. **(C)** Expression of *pcdh10* in control littermate at E16.5. **(D)** Expression of *pcdh10* in a *CNGA2*$^{-/-}$ mutant. **(E)** Pixel intensity comparison between epithelia derived from mutant and control animals. Data from three mutant/control pairs (E16.5) were examined for differences in signal intensity. *OMP* showed no significant difference in expression between mutants and controls ($p = 0.69$). *Pcdh10* expression in *CNGA2* mutants was 10% that of control ($p < 0.05$) while *kirrel2* expression was just 2% of control ($p < 0.05$). *Kirrel3* expression was approximately three times that of control, but this difference was not significant ($p = 0.31$). Scale bar = 50 μm.

PCDH10 EXPRESSION CAN BE INDUCED BY cAMP

The influence of second messenger systems on gene expression has been previously studied. These studies indicated *kirrel2/3* are regulated by cAMP in a non-PKA dependent manner. We tested whether or not *pcdh10* is similarly regulated using explant cultures derived from P0 epithelia. Explant cultures were treated with increasing concentrations of forskolin (0, 20, 40, 80 μM) for 1.5 h to drive elevated levels of cAMP. Quantitative RT-PCR showed that expression of *pcdh10* can be induced with forskolin ($n = 3$). Although the levels of induction varied from culture to culture, expression of *pcdh10* in general appeared maximal at 20 μM (representative qRT-PCR shown in **Figure 8C**). We treated explant cultures with 20 μM forskolin for 30–90 min. Western blot analysis showed a rise and fall in phosphocreb expression over this time period, indicating 1 h is likely to be optimal for exposure (**Figure 8A**).

To determine if *pcdh10* regulation by forskolin is mediated in part by PKA, we next pre-treated explants overnight with 40 μM RpcAMPs, an inhibitor of PKA. Pre-treated and control explants were then incubated with 20 μM forskolin for 1 h. Addition of RpcAMPs prior to forskolin resulted in a decrease in phosphocreb signal, consistent with inhibition of PKA (**Figure 8B**). However, qRT-PCR showed no change in *pcdh10* expression as a result of RpcAMPs pretreatment ($n = 3$; representative qRT-PCR shown

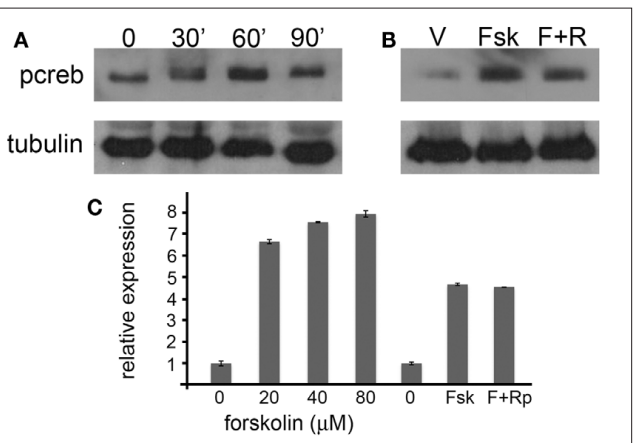

FIGURE 8 | *Pcdh10* expression is regulated by cAMP in explants. (A) *Ex vivo* culture of explants treated with 20 μM forskolin for 0, 30, 60, and 90 min results in a transient increase in phosphocreb signal. **(B)** Pretreatment of explants with 40 μM RpcAMPs overnight prior to addition of forskolin (20 μM; 1 h) reduces phosphocreb. **(C)** Representative qRT-PCR showing forskolin (20–80 μM) can induce the expression of *pcdh10* in explants relative to vehicle (DMSO) alone. Induction of *pcdh10* expression is not blocked by pretreatment with RpcAMPs.

in **Figure 8C**). These results are consistent with regulation of *pcdh10* by cAMP, but in a manner that is not dependent upon PKA. Furthermore, the observed increases in *pcdh10* expression upon addition of forskolin complement our occlusion and *CNGA2* mutant assays, which show decreases in *pcdh10* expression.

TRANSGENIC ANALYSIS OF *PCDH10* FUNCTION SHOWS AN EFFECT ON OSN AXONS

Our studies in the epithelium are consistent with regulation of *pcdh10* by activity. We next asked whether or not this regulation might affect OSN axon guidance. *Pcdh10* is clearly expressed within a mosaic population of OSNs, and its expression can be increased by cAMP or decreased by a change in activity. *Pcdh10* is a member of the cadherin superfamily, which are cell–cell adhesion molecules. If either the presence of *pcdh10* within a given OSN or the level of *pcdh10* expression is important for OSN axon–axon interactions, any alteration in *pcdh10* expression can potentially affect OSN guidance.

To test if the mosaic nature of *pcdh10* expression is important, we generated a transgenic mouse where *pcdh10* expression is under control of the *OMP* promoter (**Figure 9A**). Four independent inserts were obtained, but only two showed misexpression of *pcdh10*. Despite the use of the *OMP* promoter, we were unable to obtain general expression of *pcdh10* throughout the epithelium in either of these two inserts. Unexpectedly, both inserts had very similar expression patterns, but differed primarily by intensity of expression. While *pcdh10* misexpression does occur, it is most apparent in areas that express *pcdh10* weakly in control animals (compare **Figures 9B,C**). Areas that normally have *pcdh10* expression do not obviously over-express *pcdh10* in transgenic animals. We also performed immunohistochemistry with antibodies against *pcdh10* (**Figures 9D,E**) and *eGFP* (data not shown). Identical patterns were observed for both antibodies. Expression of *pcdh10* in the transgenic animal is significantly higher in the bulb compared controls. Strong expression of *pcdh10* could be detected in axons of P0 transgenic animals within the bulb. However, this pattern was strikingly enriched in some areas of the bulb relative to others. More expression was detected in the dorsomedial and ventral bulb than at other locations, although expression could be seen at different levels throughout the bulb. Higher magnification images showed this expression could be detected within glomeruli (**Figure 9E**).

Because of this unusual expression, we asked whether or not misexpression of *pcdh10* in these transgenic animals occurs in a differential manner across OSN populations. Using one of the two inserts with the highest level of expression, we performed double-label *in situ* hybridization with *pcdh10* and four different odorant receptors (**Figure 9F**). The percentage of OSNs expressing the *P2* or *OR78* odorant receptors and *pcdh10* is unchanged between control and transgenic animals. However, *pcdh10* is now expressed in a higher percentage of OSNs expressing the *MOR28* or *SR1* receptors. We therefore asked whether or not this misexpression influences the behavior of these OSN populations.

We crossed our transgenic line with the highest level of expression to two reporter strains. The *SR1-ires-tau-lacZ* and *P2-ires-tau-lacZ* reporters are used to study convergence of OSNs expressing the *SR1* and *P2* odorant receptors (Mombaerts et al., 1996; Cutforth et al., 2003). Our double-label experiments indicate only a small percentage of cells in either control or transgenic animals co-express the *P2* odorant receptor and *pcdh10*, consistent with *pcdh10* having no impact on these OSNs. As expected, we saw no effects

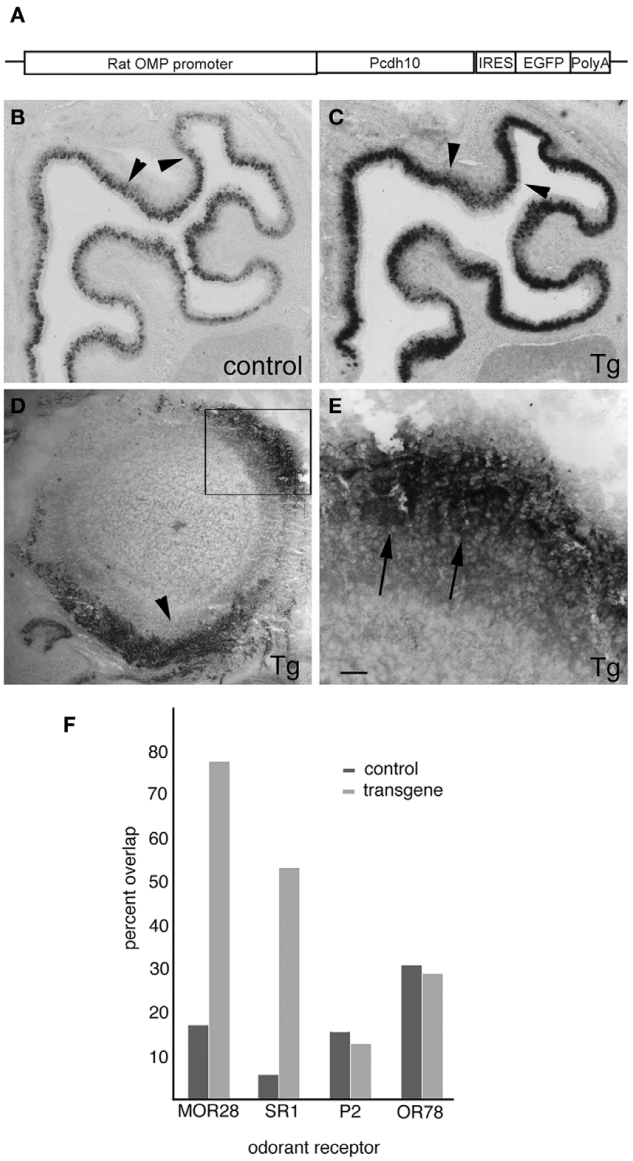

FIGURE 9 | Expression of *pcdh10* in *OMP-pcdh10* transgenic animals. (A) Schematic of the plasmid used to generate the *OMP-pcdh10* transgenic mutant. **(B)** *In situ* hybridization to detect *pcdh10* expression in control **(B)** and transgenic **(C)** animals. Note that misexpression is not uniform throughout the epithelium. Misexpression of *pcdh10* is patchy in areas where strong *pcdh10* expression is present in control animals [compare arrowheads in **(B)** and **(C)**]. **(D)** Immunohistochemical detection of *pcdh10* protein in olfactory bulbs of transgenic animals. Medial is to the right. Strong axonal and glomerular signal can be detected, but this expression is not uniform. Expression is highest along the dorsomedial and ventral aspects of the bulb (arrowhead). **(E)** Higher magnification of boxed area shown in **(D)** demonstrating protocadherin expression in glomeruli (arrowheads). Image has been rotated to better illustrate glomerular signal. **(F)** Quantitation of double-label *in situ* hybridization with *pcdh10* and *MOR28* [45/58 (Tg), 4/23 (control)], *SR1* [8/15 (Tg), 1/17 (control)], *OR78* [7/24 (Tg), 9/15 (control)], and *P2* (odorant receptors in control and transgenic animals). Scale bar = 200 μm **(B,C)**, 100 μm **(D)**, 32 μm **(E)**.

on the behavior of *P2-lacZ* OSNs in transgenic animals ($n = 16$; data not shown). Littermate controls reacted simultaneously and for identical lengths of time were compared for phenotypes with each transgenic animal. *SR1*-expressing OSNs rarely co-express *pcdh10* in control animals. However, in the mutant, a significant percentage of *SR1*-positive neurons now express *pcdh10*. The effect of this expression could clearly be seen at both E16.5 and at E17.5. In control animals at E16.5, the earliest *SR1*-expressing OSNs can clearly be seen to form small glomeruli (**Figure 10A**). However, in mutants, neurons appear to have difficulty converging ($n = 5$). Weak glomerular-like structures can be seen, but most neurons have not yet converged upon these locations (**Figure 10B**). At E17.5, the positions of target glomeruli of *SR1*-positive OSNs in mutants (**Figure 10D**; $n = 12$) appear shifted from those in controls (**Figure 10C**).

To quantify this shift, we sectioned mutant and control animals along the anterior–posterior ($n = 6$), medial–lateral ($n = 5$), and dorsal–ventral ($n = 6$) axes (**Figure 10E**). We determined the relative distance between glomeruli along all three axes in mutant and control strains. Clear differences in the relative anterior–posterior [320 ± 70 μm (Tg) vs. 520 ± 115 μm (control); $p < 0.005$] and medial–lateral [430 ± 101 μm (Tg) and 580 ± 34 μm (control); $p < 0.05$] positioning of the two glomeruli. Variable but insignificant differences in dorsal–ventral interglomerular distance are also seen [15 ± 72μm (Tg) vs. 77 ± 46 μm (control); $p = 0.09$]. Because we could not ascertain the original position of *SR1* glomeruli in the transgene, we cannot determine whether one or both glomeruli are shifted along the AP and ML axes. We repeated this analysis with the second transgenic insert. As noted previously, the overall expression pattern in the epithelium for this second insert mirrored

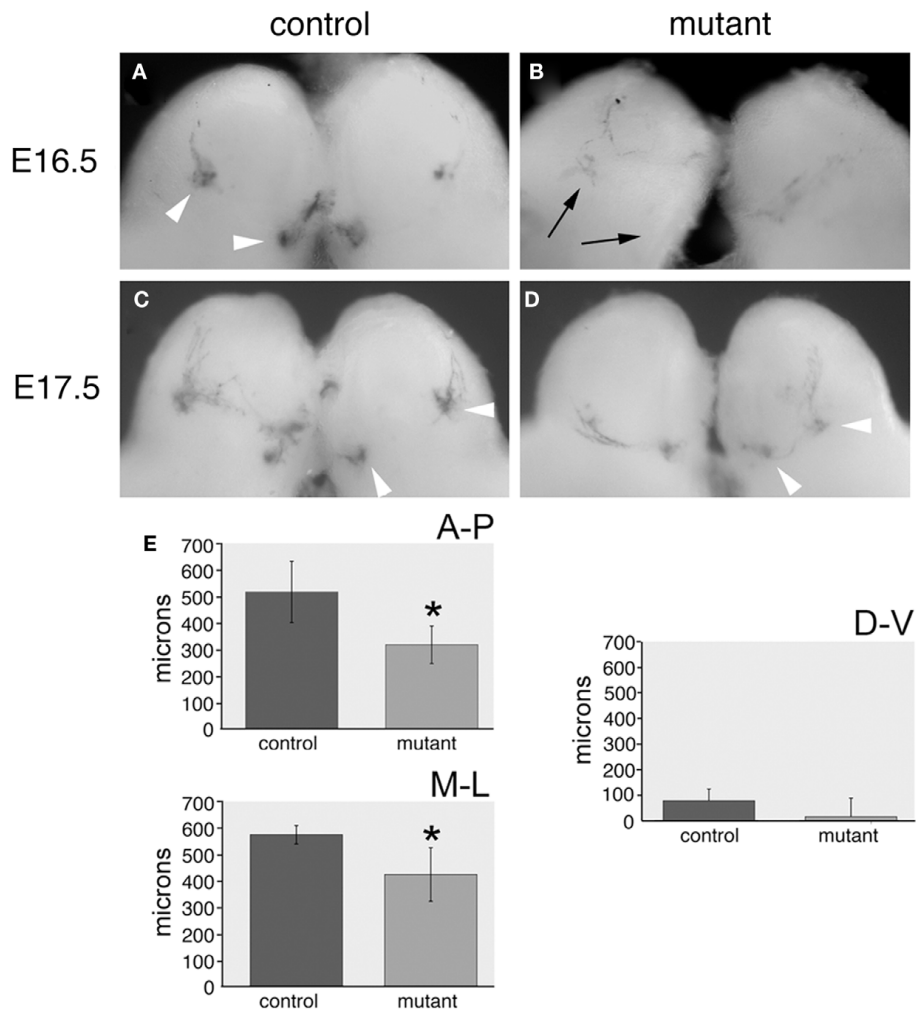

FIGURE 10 | Glomeruli of SR1-expressing OSNs in *OMP-pcdh10* mice are shifted relative to control. (A,B) E16.5 bulbs from control **(A)** and transgenic **(B)** littermates crossed with the *SR1-ires-tau-lacZ* reporter strain. Note glomerular formation (arrowheads) by *SR1*-expressing OSNs can clearly be detected in control animals while *lacZ* staining appears more diffuse in transgenic animals (black arrows point to expected location of *SR1* glomeruli). Weak glomerular-like structures can sometimes be observed near these locations. **(C)** E17.5 bulbs from control littermates show glomerular convergence to typical locations targeted by *SR1*-expressing OSNs (arrowheads). **(D)** *SR1*-positive OSNs also converge in transgenic animals, but these glomeruli appear physically closer to one another relative to control animals. **(E)** Quantitation of the convergence phenotype shows mutant glomeruli are significantly closer to one another in the anterior–posterior ($p < 0.005$) and medial–lateral dimensions ($p < 0.05$), but their relative separation is essentially unchanged along the dorsal–ventral axis.

that of our highest expressing line, but has a lower level of *pcdh10* misexpression. Although the shifts were not as dramatic as for the initial insert, statistically significant differences in anterior–posterior and medial–lateral positioning were also seen for this second insert (data not shown; $p < 0.05$).

The closer apposition of glomeruli in the transgenic animal may be due to the fact that bulb sizes in the mutant are smaller than that of controls. We sectioned bulbs from two pairs of littermates from the medial bulbar surface to the lateral-most edge. We found no differences in the total number of sections between mutant and control [56(Tg)/57(control), and 60(Tg)/59(control)]. Slight differences were found in the number of sections along the anterior/posterior extent of the bulb between mutant and control [56(Tg)/57(control), 63(Tg)/65(control), 61(Tg)/64(control)]. We cannot exclude these differences are within the realm of normal variation. We conclude *pcdh10*, like *ephrin/EphA5*, *kirrel2/3*, and *BIG2*, can affect OSN axon behavior.

DISCUSSION

How activity affects OSN guidance has long been a subject of much debate. Reduction in spontaneous OSN activity or loss-of-function mutations in the *HCN* channel both affect OSN axon guidance (Yu et al., 2004; Mobley et al., 2010). But despite disruptions in OSN behavior, the specific molecular mechanisms that underlie these phenotypes remain unknown.

In contrast, loss-of-function studies in the *CNGA2* gene showed minimal effects on OSN convergence (Lin et al., 2000), although these effects may be variable among OSN populations (Zheng et al., 2000). But unlike experiments where spontaneous or *HCN*-mediated activity was affected, a small number of genes have been identified whose expression appears to be dependent in part on the *CNG* channel. *Kirrel2/3, ephrinA5*/*EphA5*, and *BIG2* have been functionally demonstrated to be affected by loss of the *CNG* channel (Serizawa et al., 2006; Kaneko-Goto et al., 2008). Importantly, all of these genes have been shown by gain and loss-of-function studies to affect OSN terminal guidance stages. The effects of each mutation vary amongst one another. Manipulating *kirrel2*/3 expression, for example, can produce shifts of just one glomerulus within the olfactory bulb. As a result, the *CNG* channel has been proposed to be important for terminal stages of OSN guidance (Sakano, 2010). How activation of the *CNG* channel affects gene expression is still unknown. In one model, OSNs that express a common odorant receptor would respond similarly when exposed to a cognate odorant. This would lead to coordinated gene expression changes, possibly as a result of calcium entry through the channel.

Activity in the olfactory system has been proposed to also include activation of second messenger systems (Zou et al., 2009). Loss- and gain-of-function studies show altering levels of cAMP can lead to changes in OSN guidance. Early events in axonogenesis are thought to be regulated by PKA via phosphocreb, while later targeting events are thought to be regulated by activation of the *CNG* channel (Sakano, 2010). How this process occurs and how presumably subtle differences in second messenger levels are distinguished among different OSN populations is still unclear. How many genes are regulated in this manner is also unclear.

Understanding the principles that underlie this process requires identifying a sufficient cohort of genes regulated by activity. Despite the fact that only a few such genes have been shown to be affected by loss of the *CNG* channel, there are indications that multiple mechanisms may occur within this branch to regulate downstream expression. Both *BIG2* and *ephrinA5* respond similarly to loss of odorant-evoked activity. However, OSNs that express *BIG2* may or may not also express *ephrinA5*. Thus, despite the fact that both genes are similarly regulated by activity, OSNs that express *BIG2* do not necessarily express *ephrinA5* (Kaneko-Goto et al., 2008). This suggests more than one mechanism exists to regulate expression downstream of the channel to generate *BIG2*-positive/*ephrinA5*-positive or *BIG2*-positive/*ephrinA5*-negative OSNs (Imai and Sakano, 2008).

Our results show *pcdh10* is also regulated by activity. Reducing odorant-evoked activity, either by naris occlusion or by a mutation in the *CNGA2* channel, leads to reduced *pcdh10* expression. *Ex vivo* manipulation of cAMP levels in explants can lead to elevated *pcdh10* expression, and this increase is not dependent upon PKA. The identification of *pcdh10* complements and extends prior studies identifying *kirrels*, *ephrin/EphA5*, and *BIG2* as regulators of OSN axon guidance. Like *kirrel2*, *pcdh10*-positive axons correlate with those expressing *CNGA2,* and both *pcdh10* and *kirrel2* are similarly affected by changes in activity. However, there are suggestions that, like *BIG2*, more than one mechanism regulates gene expression downstream of the *CNG* channel. We found that essentially all OSNs that express *pcdh10* also express *kirrel2*. However, the converse is not true, as only a subset of *kirrel2*-positive OSNs express *pcdh10*. This demonstrates the presence of two distinct *kirrel2* populations (*kirrel2*-positive/*pcdh10*-positive and *kirrel2*-positive/*pcdh10*-negative OSNs). This argues that, much as there are two populations of *BIG2*-positive OSNs, more than one mechanism may exist to regulate *pcdh10* expression within these OSNs.

How do these two *kirrel2* populations arise, if both *pcdh10* and *kirrel2* are similarly regulated by activity? During tumorigenesis, *pcdh10* expression is known to be affected by methylation (Lin et al., 2010). It is possible that an epigenetic mechanism may initially regulate the presence or absence of *pcdh10* in a given OSN. Regulation of expression by activity would therefore be a secondary event that could only occur in OSNs that express *pcdh10.* Alternatively, activity-regulated expression of *pcdh10* may require some minimum level of activity to be effective, and this threshold may be higher than that of *kirrel2*. In this scenario, *kirrel2* can be widely expressed by many OSN populations. However, *pcdh10* expression in these populations would be more dependent upon prolonged or elevated levels of activity.

What is the purpose of this regulation of *pcdh10* expression by activity? The mosaic nature of *pcdh10* expression suggests a possible role in OSN axon guidance. The absence of *pcdh10* expression by *in situ* hybridization prior to E15.5 indicates *pcdh10* is not involved in early stages of OSN outgrowth. Moreover, the presence of *pcdh10* expression in axons and within glomeruli increases as postnatal development proceeds. These expression patterns are consistent with a role in later stages of OSN guidance, possibly during glomerular refinement and/or synaptogenesis. *Kirrel2*/3 are also theorized to be involved in terminal stages of axon guidance. It

is clear, however, given the sheer number of glomeruli, that multiple guidance cues must be involved at this stage. The differing expression of *pcdh10* among *kirrel2*-positive neurons may enable these neurons to further discriminate among terminal glomerular positions within the bulb.

Consistent with a model where activity-dependent mechanisms mediate terminal targeting and refinement of glomerular positioning, we found that *kirrel2*, *kirrel3*, and *pcdh10* overlapped significantly in expression among OSNs at birth. This overlap was gradually reduced over the first 2.5 weeks of life, in keeping with the glomerular refinement known to occur during postnatal stages. Somewhat unexpectedly, we also saw changes in both *kirrel2* and *pcdh10* at E16.5 in *CNGA2* mutants. At this stage, glomerular convergence has just begun for OSNs expressing *SR1* (e.g., **Figure 9**). These results suggest that activity via the *CNG* channel may occur earlier than expected to regulate gene expression.

At E17.5, OSN terminal targeting in our transgenic mutant appeared to be shifted along the anterior–posterior and medial–lateral axes. Although subtle, these shifts are similar to those observed for *kirrel2/3*, where bulbar positioning is shifted by a single glomerulus. We note that *pcdh10*, like other protocadherins, exhibits only weak adhesive properties *in vitro* (Hirano et al., 1999). It seems unlikely that homophilic interactions among OSNs expressing *pcdh10* can explain these observed phenotypes. However, *pcdh10* has been shown to negatively regulate other guidance cues, such as *N-cadherin* (Nakao et al., 2008). In these studies, co-expression of *pcdh10* and *N-cadherin* in a tissue culture model led to down-regulation of *N-cadherin* expression at the surface. Thus, our experiments mis-expressing *pcdh10* are likely to impact the expression of other guidance cues, and suggest that regulation of one gene by activity can in fact influence others that are not similarly regulated.

Finally, we note that *pcdh10* has been implicated as being regulated by activity in the hippocampus (Morrow et al., 2008). The *CNG* channel is also expressed in hippocampal neurons (Bradley et al., 1997). It is possible regulation of *pcdh10* expression in these two structures may operate through similar mechanisms. Other members of the *delta* protocadherin family are thought to be regulated by activity. *Arcadlin*, an ortholog of *pcdh8*, is up-regulated in the hippocampus in response to electroshock treatment (Yasuda et al., 2007) while *pcdh9* is up-regulated in response to *creb* (Zhang et al., 2009). These studies indicate that understanding regulation of protocadherin expression by activity in the olfactory system may have broader implications for understanding this regulation elsewhere in the nervous system.

ACKNOWLEDGMENTS

We thank Mark Roberson for guidance on the pharmacology assays. This work was funded by the NIH (DC007489) and the Cornell Nanobiotechnology Center.

SUPPLEMENTARY MATERIAL

The Supplementary Material for this article can be found online at http://www.frontiersin.org/Neural_Circuits/10.3389/fncir.2011.00009/abstract/

MOVIE S1 | Three-dimensional reconstruction of *pcdh10* glomerular map. The movie begins with the anterior view displayed in Figure 3A. Dorsal is up, medial to the left, ventral is down, and lateral to the right. As the movie progresses the glomerular map rotates in the medioventral direction, displaying medial, posterior, and finally lateral views of *pcdh10*-positive glomeruli.

REFERENCES

Aoki, E., Kimura, R., Suzuki, S. T., and Hirano, S. (2003). Distribution of OL-protocadherin protein in correlation with specific neural compartments and local circuits in the postnatal mouse brain. *Neuroscience* 117, 593–614.

Bradley, J., Zhang, Y., Bakin, R., Lester, H. A., Ronnett, G. V., and Zinn, K. (1997). Functional expression of the heteromeric "olfactory" cyclic nucleotide-gated channel in the hippocampus: a potential effector of synaptic plasticity in brain neurons. *J. Neurosci.* 17, 1993–2005.

Cutforth, T., Moring, L., Mendelsohn, M., Nemes, A., Shah, N. M., Kim, M. M., Frisen, J., and Axel, R. (2003). Axonal ephrin-As and odorant receptors: coordinate determination of the olfactory sensory map. *Cell* 114, 311–322.

Hirano, S., Yan, Q., and Suzuki, S. T. (1999). Expression of a novel protocadherin, OL-protocadherin, in a subset of functional systems of the developing mouse brain. *J. Neurosci.* 19, 995–1005.

Imai, T., and Sakano, H. (2008). Odorant receptor-mediated signaling in the mouse. *Curr. Opin. Neurobiol.* 18, 251–260.

Imai, T., Suzuki, M., and Sakano, H. (2006). Odorant receptor-derived cAMP signals direct axonal targeting. *Science* 314, 657–661.

Kaneko-Goto, T., Yoshihara, S., Miyazaki, H., and Yoshihara, Y. (2008). BIG-2 mediates olfactory axon convergence to target glomeruli. *Neuron* 57, 834–846.

Lin, C. J., Lai, H. C., Wang, K. H., Hsiung, C. A., Liu, H. W., Ding, D. C., Hsieh, C. Y., and Chu, T. Y. (2010). Testing for methylated PCDH10 or WT1 is superior to the HPV test in detecting severe neoplasms (CIN3 or greater) in the triage of ASC-US smear results. *Am. J. Obstet. Gynecol.* 204, 21.

Lin, D. M., Wang, F., Lowe, G., Gold, G. H., Axel, R., Ngai, J., and Brunet, L. (2000). Formation of precise connections in the olfactory bulb occurs in the absence of odorant-evoked neuronal activity. *Neuron* 26, 69–80.

Mobley, A. S., Miller, A. M., Araneda, R. C., Maurer, L. R., Muller, F., and Greer, C. A. (2010). Hyperpolarization-activated cyclic nucleotide-gated channels in olfactory sensory neurons regulate axon extension and glomerular formation. *J. Neurosci.* 30, 16498–16508.

Mombaerts, P., Wang, F., Dulac, C., Chao, S. K., Nemes, A., Mendelsohn, M., Edmondson, J., and Axel, R. (1996). Visualizing an olfactory sensory map. *Cell* 87, 675–686.

Morrow, E. M., Yoo, S. Y., Flavell, S. W., Kim, T. K., Lin, Y., Hill, R. S., Mukaddes, N. M., Balkhy, S., Gascon, G., Hashmi, A., Al-Saad, S., Ware, J., Joseph, R. M., Greenblatt, R., Gleason, D., Ertelt, J. A., Apse, K. A., Bodell, A., Partlow, J. N., Barry, B., Yao, H., Markianos, K., Ferland, R. J., Greenberg, M. E., and Walsh, C. A. (2008). Identifying autism loci and genes by tracing recent shared ancestry. *Science* 321, 218–223.

Nakao, S., Platek, A., Hirano, S., and Takeichi, M. (2008). Contact-dependent promotion of cell migration by the OL-protocadherin-Nap1 interaction. *J. Cell Biol.* 182, 395–410.

Redies, C., Vanhalst, K., and Roy, F. (2005). Delta-protocadherins: unique structures and functions. *Cell. Mol. Life Sci.* 62, 2840–2852.

Rodriguez, S., Sickles, H. M., Deleonardis, C., Alcaraz, A., Gridley, T., and Lin, D. M. (2008). Notch2 is required for maintaining sustentacular cell function in the adult mouse main olfactory epithelium. *Dev. Biol.* 314, 40–58.

Ronnett, G. V., Hester, L. D., and Snyder, S. H. (1991). Primary culture of neonatal rat olfactory neurons. *J. Neurosci.* 11, 1243–1255.

Sakano, H. (2010). Neural map formation in the mouse olfactory system. Neuron 67, 530–542.

Serizawa, S., Miyamichi, K., Takeuchi, H., Yamagishi, Y., Suzuki, M., and Sakano, H. (2006). A neuronal identity code for the odorant receptor-specific and activity-dependent axon sorting. *Cell* 127, 1057–1069.

Todrank, J., Heth, G., and Restrepo, D. (2011). Effects of in utero odorant exposure on neuroanatomical development of the olfactory bulb and odour preferences. *Proc. Biol. Sci.* 278, 1949–1955.

Uemura, M., Nakao, S., Suzuki, S. T., Takeichi, M., and Hirano, S. (2007). OL-protocadherin is essential for growth of striatal axons and thalamocortical projections. *Nat. Neurosci.* 10, 1151–1159.

Williams, E. O., Xiao, Y., Sickles, H. M., Shafer, P., Yona, G., Yang, J. Y., and Lin, D. M. (2007). Novel subdomains

of the mouse olfactory bulb defined by molecular heterogeneity in the nascent external plexiform and glomerular layers. *BMC Dev. Biol.* 7, 48. doi: 10.1186/1471-213X-7-48

Yasuda, S., Tanaka, H., Sugiura, H., Okamura, K., Sakaguchi, T., Tran, U., Takemiya, T., Mizoguchi, A., Yagita, Y., Sakurai, T., De Robertis, E. M., and Yamagata, K. (2007). Activity-induced protocadherin arcadlin regulates dendritic spine number by triggering N-cadherin endocytosis via TAO2beta and p38 MAP kinases. *Neuron* 56, 456–471.

Yu, C. R., Power, J., Barnea, G., O'donnell, S., Brown, H. E., Osborne, J., Axel, R., and Gogos, J. A. (2004). Spontaneous neural activity is required for the establishment and maintenance of the olfactory sensory map. *Neuron* 42, 553–566.

Zhang, S. J., Zou, M., Lu, L., Lau, D., Ditzel, D. A., Delucinge-Vivier, C., Aso, Y., Descombes, P., and Bading, H. (2009). Nuclear calcium signaling controls expression of a large gene pool: identification of a gene program for acquired neuroprotection induced by synaptic activity. *PLoS Genet.* 5, e1000604. doi: 10.1371/journal.pgen.1000604

Zhao, H., and Reed, R. R. (2001). X inactivation of the OCNC1 channel gene reveals a role for activity-dependent competition in the olfactory system. Cell 104, 651–660.

Zheng, C., Feinstein, P., Bozza, T., Rodriguez, I., and Mombaerts, P. (2000). Peripheral olfactory projections are differentially affected in mice deficient in a cyclic nucleotide-gated channel subunit. *Neuron* 26, 81–91.

Zou, D. J., Chesler, A., and Firestein, S. (2009). How the olfactory bulb got its glomeruli: a just so story? *Nat. Rev. Neurosci.* 10, 611–618.

Zou, D. J., Chesler, A. T., Le Pichon, C. E., Kuznetsov, A., Pei, X., Hwang, E. L., and Firestein, S. (2007). Absence of adenylyl cyclase 3 perturbs peripheral olfactory projections in mice. *J. Neurosci.* 27, 6675–6683.

Conflict of Interest Statement: The authors declare that the research was conducted in the absence of any commercial or financial relationships that could be construed as a potential conflict of interest.

Received: 02 April 2011; accepted: 26 July 2011; published online: 23 August 2011.
Citation: Williams EO, Sickles HM, Dooley AL, Palumbos S, Bisogni AJ and Lin DM (2011) Delta protocadherin 10 is regulated by activity in the mouse main olfactory system. Front. Neural Circuits. 5:9. doi: 10.3389/fncir.2011.00009